Widths of astrophysically important resonances in ^{18}Ne

B. Harss,* C. L. Jiang, K. E. Rehm, J. P. Schiffer, J. Caggiano, P. Collon, J. P. Greene, D. Henderson, A. Heinz, R. V. F. Janssens, J. Nolen, R. C. Pardo, T. Pennington, R. H. Siemssen, A. A. Sonzogni, J. Uusitalo, and I. Wiedenhöver
Argonne National Laboratory, Argonne, Illinois 60439

M. Paul
Hebrew University, Jerusalem, Israel

T. F. Wang
Lawrence Livermore National Laboratory, Livermore, California 94550

F. Borasi and R. E. Segel
Northwestern University, Evanston, Illinois 60208

J. C. Blackmon and M. Smith
Physics Division, Oak Ridge National Laboratory, Oak Ridge, Tennessee 37831-6354

A. Chen and P. Parker
Wright Nuclear Structure Laboratory, Yale University, New Haven, Connecticut 06520-8124
(Received 27 September 2001; published 22 February 2002)

The astrophysically important reaction $^{14}O(\alpha,p)^{17}F$ has been studied through a measurement of the time-inverse $p(^{17}F,\alpha)^{14}O$ reaction using a radioactive ^{17}F beam. Resonance parameters for several states above an excitation energy of 7 MeV in ^{18}Ne have been obtained. Through a measurement of the partial widths for elastic and inelastic proton scattering, it was determined that for these resonances the contribution of the $^{14}O(\alpha,p)^{17}F^*$ branch populating the first excited state in ^{17}F is small. The results indicate that the contribution of resonances above $E_x = 7$ MeV to the astrophysical (α,p) reaction rate is smaller than was previously assumed.

DOI: 10.1103/PhysRevC.65.035803 PACS number(s): 25.60.Bx, 25.60.Je, 26.30.+k

I. INTRODUCTION

The level structure of ^{18}Ne above the proton threshold at 3.92 MeV influences a variety of astrophysical processes [1,2]. In stellar explosions, such as novae and x-ray bursts, ^{14}O is produced via the $^{13}N(p,\gamma)^{14}O$ reaction which bypasses the slow β decay of ^{13}N ($T_{1/2}=9.96$ m). The β decay of ^{14}O ($T_{1/2}=70.6$ s) can only be bypassed by the $^{14}O(\alpha,p)^{17}F$ reaction, which proceeds through resonant states in ^{18}Ne. Starting with $^{17}F(p,\gamma)^{18}Ne$, going again through resonant states in ^{18}Ne [3], a network of nuclear reactions can generate nuclei with masses $A>17$. At the extreme temperatures found in x-ray bursts ($T\sim 2\times 10^9$ K) states in ^{18}Ne with excitation energies above 7 MeV may contribute significantly to the reaction rate. Some information about these states was recently reported [4,5]. In Ref. [5], three resonances at $E_x=7.16\pm0.15$, 7.37 ± 0.06, and 7.62 ± 0.05 MeV had been observed and spin values were suggested. These spin values were later questioned in Ref. [6], mainly on the basis of the Coulomb shifts with respect to the analog states in the mirror nucleus ^{18}O.

A direct measurement of the excitation function for the $^{14}O(\alpha,p)^{17}F$ reaction is difficult because, in addition to a low-energy radioactive ^{14}O beam, it also requires the use of a ^{4}He gas target. Using detailed balance this reaction can also be studied via the time-inverse $^{17}F(p,\alpha)^{14}O$ reaction. This reaction, however, only provides values for the partial widths, Γ_α and Γ_p, connecting the resonance with the ground states of ^{14}O and ^{17}F, respectively. Since in an astrophysical environment the $^{14}O(\alpha,p)^{17}F$ reaction can also populate the first-excited $\frac{1}{2}^+$ state in ^{17}F at $E_x=0.495$ MeV, the partial width $\Gamma_{p'}$ must also be determined.

In this experiment, the excitation functions for elastic and inelastic scattering of protons on ^{17}F were measured in the energy range $E_{\text{c.m.}}=3.07-3.94$ MeV and proton partial widths for decay to the ground state and first-excited state in ^{17}F were determined. In addition, the measurement of the excitation function for the $^{17}F(p,\alpha)^{14}O$ reaction, previously published in Ref. [5], has been extended towards higher energies. The present data provide new information on the spins of higher-lying states in ^{18}Ne.

II. EXPERIMENTAL DETAILS

The experiment was performed at the ATLAS accelerator at Argonne National Laboratory with a ^{17}F beam produced with the in-flight technique which is described in more detail in Ref. [7]. A primary beam of ^{16}O with energies between 80 and 90 MeV bombarded a liquid-nitrogen-cooled, 3.5-cm-long gas cell, filled with $\approx$0.8 atm of D_2 gas. A few percent

*Also at Physics Department E12, Technische Universität München, München, Germany.

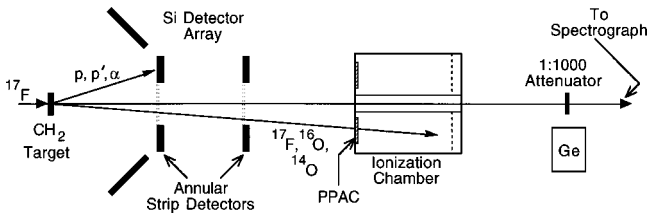

FIG. 1. Schematic of the experimental setup used for the measurement of the $^{17}F(p,p)^{17}F$ and $^{17}F(p,\alpha)^{14}O$ excitation functions. The heavy particles (^{17}F, ^{16}O, ^{14}O) were identified in an annular gas detector covering the angle range $\theta_{lab}=1.5-6.5°$. The coincident light particles (protons and alphas) were detected in an array consisting of two annular Si detectors covering the range $\theta_{lab}=7-24.5°$ and six Si strip detectors covering the range $\theta_{lab}=32-56.5°$. See text for details.

of the ^{17}F ions produced via the $d(^{16}O,^{17}F)n$ reaction were accepted by the 16-m-long beam transport system and focussed onto a 5×5-mm^2 spot. The transport system consisted of a superconducting solenoid mounted directly after the production target, a superconducting resonator to focus the particles in energy, and a 22° bending magnet for separation of the $^{17}F^{+9}$ ions from the primary ^{16}O beam. Between 10^5 and 10^6 ^{17}F/sec [$E(^{17}F)=54.8-70.3$ MeV] were incident on the secondary target with a 0.5–1-MeV energy spread (30–60 keV in the center-of-mass system). Contamination from the tails of the primary ^{16}O beam particles, which have the same magnetic rigidity (and thus lower energy), varied between 10 and 500% and was monitored continuously with an Enge split-pole magnetic spectrograph and its associated focal plane detector [8] located at 0°. Because the energy of the ^{16}O particles was about 10 MeV below that of the ^{17}F beam, reactions induced by ^{16}O could easily be separated.

The $p(^{17}F,p)^{17}F$ and $p(^{17}F,\alpha)^{14}O$ reactions were measured at a number of incident energies, covering the c.m. energy range of 3.07–3.94 MeV. Polypropylene $(CH_2)_n$ targets with thicknesses of ~100 μg/cm^2 were used. Each measurement represents an average over the 0.7 MeV (40 keV in the c.m. system) energy loss in the target, convoluted with the energy spread of the beam.

In order to separate the scattering of ^{17}F from scattering of the ^{16}O beam contaminant, the two outgoing reaction products were detected in kinematic coincidence. The heavy particles (^{17}F, ^{16}O, or ^{14}O) were identified with respect to nuclear charge Z and energy in an annular gas detector consisting of a parallel plate avalanche counter followed by a Bragg-curve ionization chamber (see Fig. 1). This detector covered the angular range $\theta_{lab}=1.5-6.5°$. The coincident protons or alphas were measured with a solid-state detector

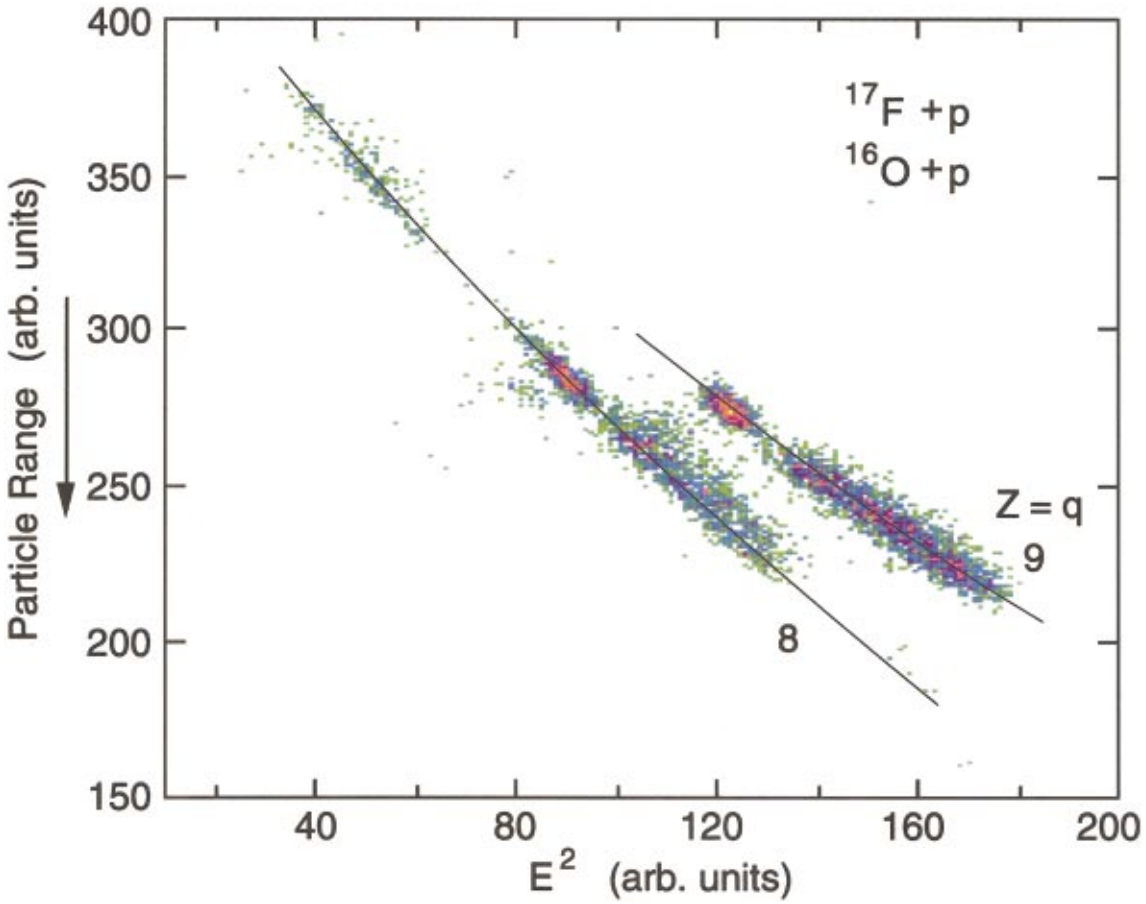

FIG. 2. (Color) Scatter plot of particle range vs E^2 measured in the Bragg curve ionization chamber. The two groups originating from the F ($Z=9$) and O ($Z=8$) components of the beam elastically scattered off the CH_2 target are clearly separated.

array consisting of two double-sided, annular silicon strip detectors covering the angular range $\theta_{lab}=7-24.5°$. These detectors were segmented into 16 rings on the front face and 16 wedges on the back face. For the (p,α) reaction this angular range corresponds to a c.m. region of $\theta_{cm}=26-165°$. The total detection efficiency was ~65%, obtained from a Monte Carlo calculation assuming an isotropic angular distribution, and including effects of a finite beam spot and multiple scattering in the target. For a measurement of elastic and inelastic scattering six additional 5×5-cm^2 Si strip detectors with a strip width of 2 mm covered the angular range $\theta_{lab}=32-56.5°$. A schematic of the experimental setup is shown in Fig. 1.

The intensity of the incident beam was monitored by two techniques:

(i) ^{17}F particles elastically scattered by carbon nuclei in the CH_2 target were detected in the ionization chamber. Assuming Rutherford scattering in the angular range of the detector ($\theta=1.5-6.5°$), the ^{17}F beam intensity could be calculated.

(ii) In addition, the decay of the ^{17}F particles stopped on a multi-pin-hole beam attenuator located in front of the magnetic spectrograph (more than 99% of the total beam intensity) were monitored with a Ge detector, positioned 20 cm away, through the 511-keV annihilation radiation. The detection efficiency for this detector was determined with a calibrated ^{68}Ge β^+ source which has an endpoint energy similar to the one of ^{17}F. The ^{68}Ge source was deposited on a stainless steel foil of the same thickness as the beam attenuator. The two techniques for measuring the beam normalization agreed to within $\pm20\%$.

Figure 2 presents a particle identification spectrum obtained with the Bragg-curve ionization chamber at a bombarding energy of 67 MeV. The contributions from the F ($Z=9$) and O ($Z=8$) components are clearly separated. By selecting events with $Z=9$ or 8, respectively, kinematic plots of angle versus energy are obtained for events in which a coincident particle is detected in the Si strip detector array [see Figs. 3(a) and (b)]. These plots clearly show events lying on the kinematic curves expected for the $p(^{17}\mathrm{F},p)^{17}\mathrm{F}$ and $p(^{16}\mathrm{O},p)^{16}\mathrm{O}$ reactions. These curves are indicated in the figures by thin solid lines. Protons with energies exceeding 6.2 MeV are not stopped in the 300-μm-thick Si strip detector. This results in a ''kink'' of the kinematic curves. Events attributed to the $p(^{17}\mathrm{F},\alpha)^{14}\mathrm{O}$ reaction were also observed at higher energies by gating on $Z=8$ events in the Bragg ionization chamber [see Fig. 3(c)]. Because all the coincident α particles are stopped in the Si detector, no kinks are observed in the kinematic curve for the (p,α) reaction.

Protons from inelastic scattering fall on kinematic curves very close to those for elastic scattering. In order to illustrate how they can be distinguished in favorable cases, Fig. 4 presents an energy spectrum for elastic scattering of $^{17}\mathrm{F}+p$ measured at a scattering angle of ~65° in the center-of-mass system ($\theta_{lab}=52.5-56.5°$). The satellite structure next to the strong elastic peak, which is not observed in the $^{16}\mathrm{O}+p$

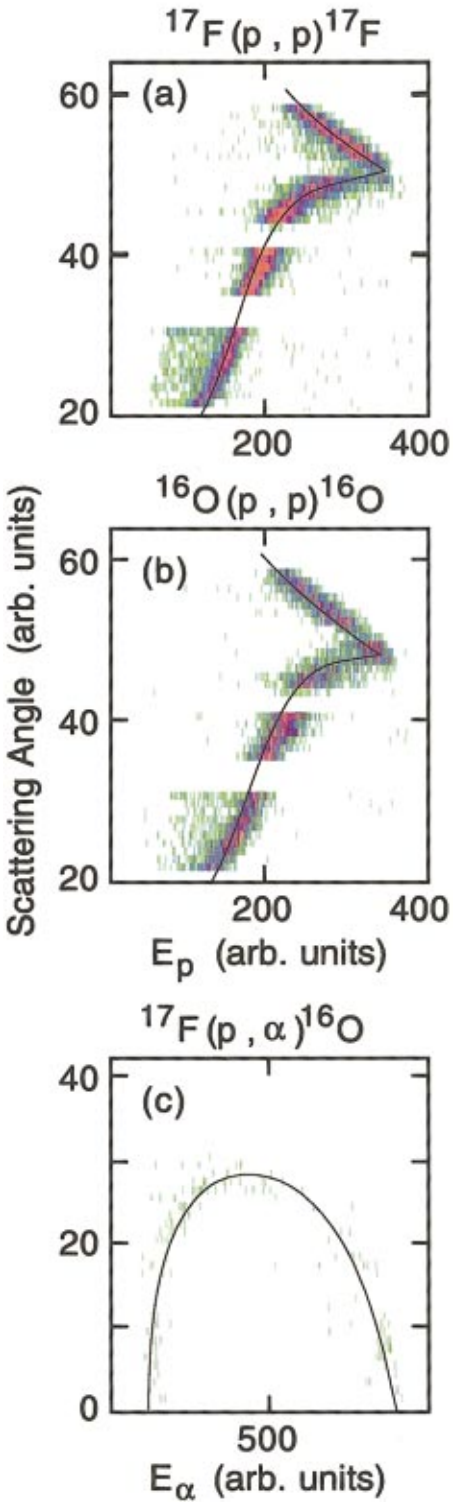

FIG. 3. (Color) Scatter plots of scattering angle (ring number) vs energy for particles detected in the Si detector array in coincidence with ^{17}F (top), ^{16}O (middle), and ^{14}O (bottom). The thin solid lines are the kinematic curves expected for elastic scattering $^{17}\mathrm{F}(p,p)^{17}\mathrm{F}$ (top), $^{16}\mathrm{O}(p,p)^{16}\mathrm{O}$ (middle), and for the $^{17}\mathrm{F}(p,\alpha)^{14}\mathrm{O}$ reaction (bottom).

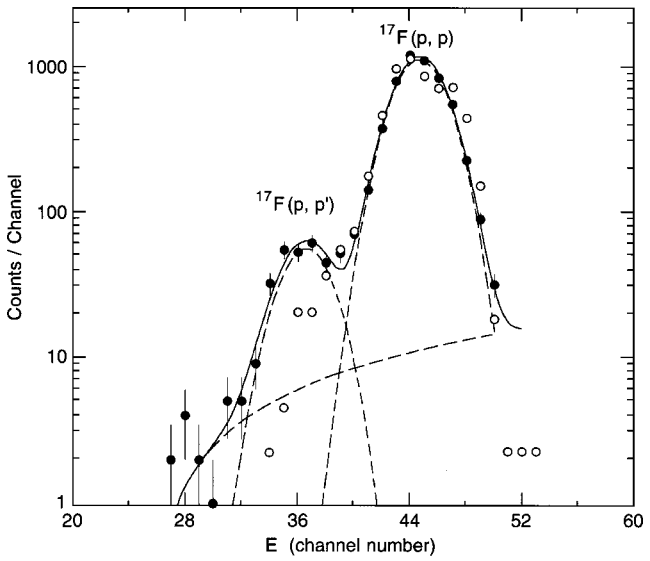

FIG. 4. Solid points: Energy spectrum measured for the ^{17}F $+p$ system at $\theta_{cm}=65°$. Open points: energy spectrum obtained for the ^{16}O$+p$ system. The latter spectrum has been shifted to coincide with the ^{17}F$+p$ spectrum. The solid and dashed lines were obtained from a least-squares fit assuming two Gaussians and a linear background.

channel, is attributed to inelastic excitation of the $\frac{1}{2}^+$ state in ^{17}F at 0.495 MeV. Despite the intrinsic energy resolution of 450 keV (mainly limited by the geometry of the detectors), a separation of the elastic and inelastic scattering events was possible since the two groups representing transitions to the ground and first-excited states in ^{17}F are separated in laboratory energy by almost 1 MeV. Since at smaller angles the energy of the elastically scattered protons exceeds 6.2 MeV the protons are not stopped in the Si detector and thus inelastic scattering events could only be extracted at the larger scattering angles.

III. EXPERIMENTAL RESULTS AND DISCUSSION

A. Elastic scattering

The level scheme of ^{18}Ne has been studied previously with several reactions, among them ^{16}O(^{3}He,n), ^{20}Ne(p,t), and ^{12}O(^{12}O, ^{6}He). Results of these experiments are summarized in Ref. [4] and the deduced level schemes are shown in Fig. 5. The main difference in the level scheme of Ref. [4] compared to that given in the compilations in Ref. [9] is in the spin assignment of a doublet of states at an excitation energy of $E_x\sim 6.3$ MeV and two new levels at $E_x=7.12$, and 7.62 MeV. The state at $E_x=7.35$ MeV, was tentatively assigned in Ref. [4] to have $J^\pi=1^-$.

Our first measurement of the ^{17}F(p,α)^{14}O reaction [5] with a radioactive ^{17}F beam found that the main (p,α) strength lies at an excitation energy of $E_x=7.60\pm0.05$ MeV with a resonance strength $\omega\gamma=300$ eV, while the strength of a state at 7.37 MeV is about a factor of 10 smaller. At 7.16 ± 0.15 MeV another structure with a small resonance strength was identified as well. However, because this energy range was covered only with a thick target in the

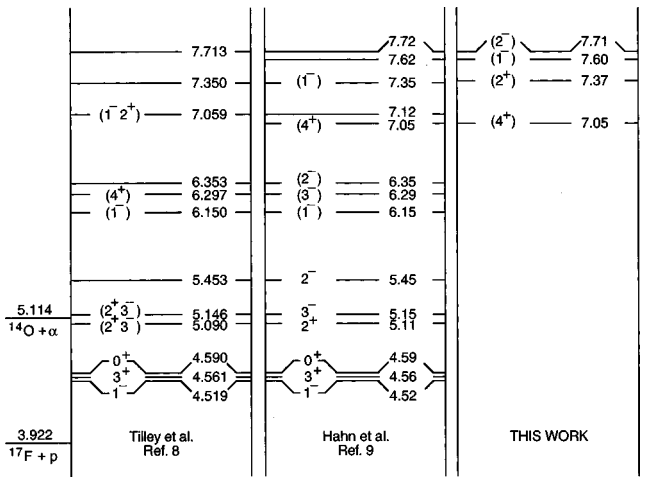

FIG. 5. Level scheme of ^{18}Ne from Ref. [9] (left) and Ref. [4] (middle) in comparison with the results obtained in this work (right). Only states above $E_x=7$ MeV are shown in the latter case.

experiment of Ref. [5], the excitation energy could be determined only with a relatively large uncertainty of ±150 keV. Based on these results and on Coulomb-shift arguments, tentative spin assignments of 1^- (7.16 MeV) 1^-, 4^+ (7.37 MeV), and 1^-, 2^+, 3^- (7.60 MeV) were proposed for these states in Ref. [5]. These assignments were later questioned in Ref. [6] arguing that the 7.60- and 7.37-MeV levels in ^{18}Ne cannot be given a $J^\pi=4^+$ assignment nor could the 7.16- and 7.37-MeV levels have spin parity of 1^-.

It was not possible in Ref. [5] to determine the spin on the basis of angular distribution measurements of the ^{17}F(p,α)^{14}O reaction, because marked differences in the distributions occur mainly at the most forward or backward angles, requiring data with high statistics that are difficult to obtain with present beam intensities. In addition, interference effects (e.g., between $l=1$ and $l=3$ transfers populating a 1^- state in ^{18}Ne) strongly influence the shape of the angular distribution. Test calculations within the formalism of Ref. [10], however, indicated that measurements of the ^{17}F(p,p)^{17}F excitation function would be more sensitive to the spin values suggested in Ref. [5]. This is shown in Fig. 6, where calculations are displayed for the excitation function at $\theta_{cm}=142°$ for a state at $E_x=7.05$ MeV with spin-parity assumptions of 1^-, 2^+, 3^-, and 4^+. It is clear that a measurement of an excitation function for elastic scattering at backward angles can readily differentiate between the $J^\pi=1^-$ and 4^+ possibilities.

The results for the measured elastic-scattering excitation functions at $\theta_{cm}=72$ and 142°, respectively, are presented in Fig. 7. At backward angles ($\theta=142°$), a peak in the cross sections around $E_p=3.13$ MeV is observed. From a comparison with calculations for $J^\pi=1^-$ and 4^+ (see solid and dashed lines in Fig. 7) a much better agreement is achieved for a 4^+ spin assignment (see Sec. III E). The value for the excitation energy ($E_x=7.05$ MeV) agrees within the experimental uncertainties with the earlier result [5] from the (p,α) reaction obtained in a thick target measurement. At forward angles the structure is much less pronounced, but consistent with this assignment.

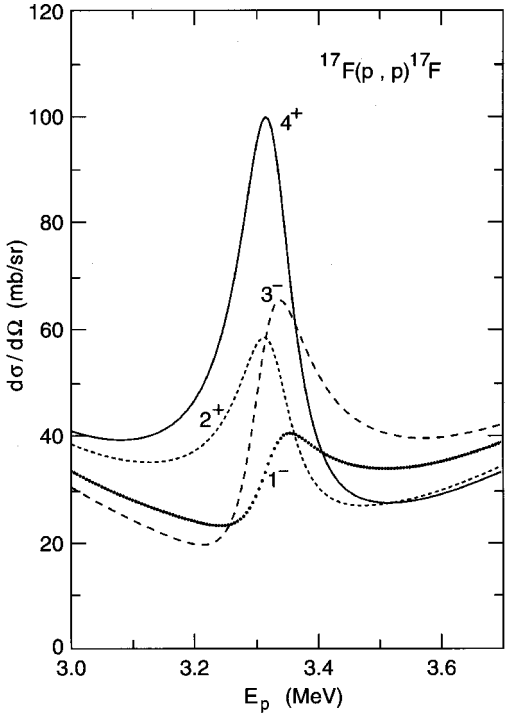

FIG. 6. Calculated excitation functions for elastic scattering populating a state at 7.05 MeV with spins 1^-, 2^+, 3^-, and 4^+. E_p is the proton energy in the laboratory system. See text for details.

The region around $E_p = 3.7$ MeV corresponding to an excitation energy of 7.37 MeV was not covered in the present measurement. The excitation energy region around $E_p = 3.9$ MeV ($E_x = 7.60$ MeV) is somewhat more complex. While at backward angles an increase in cross section by about 50% is observed, the excitation function is quite featureless in this energy range. Because of the large uncertainties in the ^{17}F(p,p) ^{17}F cross sections, no spin-parity assignments are possible in this energy region.

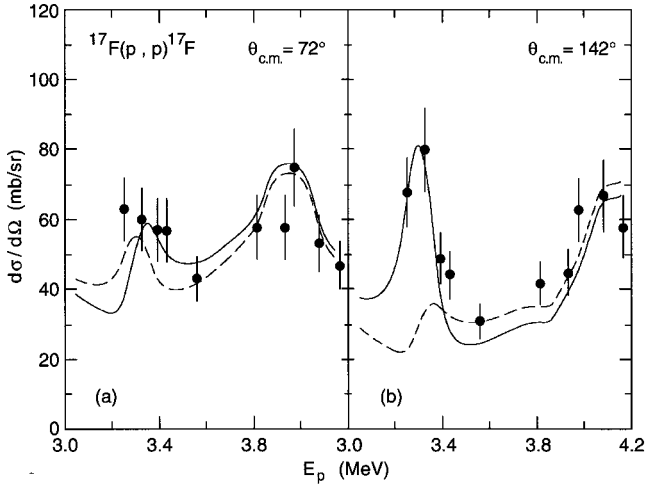

FIG. 7. Excitation functions for elastic scattering measured for the system ^{17}F$+p$ at scattering angles of $\theta_{cm} = 72$ and 142°, respectively. E_p is the proton energy in the laboratory system. The solid and dashed lines are calculated using the parameters given in Table II. See text for details.

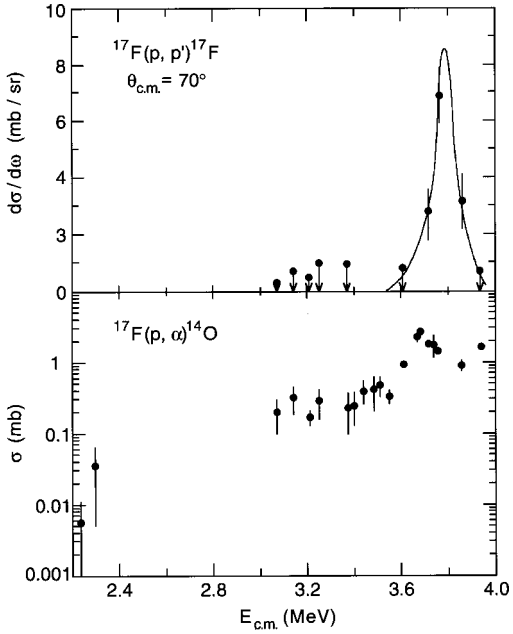

FIG. 8. Top: Differential cross section for inelastic scattering populating the first excited state in ^{17}F at $E_x = 0.495$ MeV, measured at scattering angles of $\theta_{lab} = 52.5–56.5°$. Bottom: angle-integrated cross sections for the ^{17}F$(p,\alpha)^{14}$O reaction obtained in Ref. [5] and in this work. The solid line for the excitation function of inelastic scattering serves to guide the eye.

B. Inelastic scattering ^{17}F(p,p') ^{17}F$(1/2^+)$

The excitation function measured in the angular range $\theta_{lab} = 52.5–56.5°$ is presented in the top part of Fig. 8, together with the (angle-integrated) excitation function for the ^{17}F(p,α) ^{14}O reaction. While for the cross sections in the energy region around $E_{cm} = 3.2$ MeV only upper limits of ~0.5–1 mb/sr can be given, a resonantlike structure is observed at $E_{cm} = 3.8$ MeV ($E_x = 7.71 \pm 0.05$ MeV). This structure does not show up in the measurements of the (p,α) excitation function, but coincides with a 7.71-MeV state seen in ^{12}C(^{12}C, ^{6}He) [4]. The width of this state (~70 keV) requires a low orbital angular momentum ($l \leqslant 2$) for both incident and outgoing channels and restricts the spin-parity choice for this structure to small spin values (0^+, 1^{+-}, 2^{+-}, and 3^+). The fact that no strong yield is observed for the (p,α) reaction in the corresponding energy range suggests unnatural parity for this state, i.e., 1^+, 2^-, or 3^+. Since there is a 2^- state in the mirror nucleus ^{18}O at $E_x = 7.77$ MeV, the structure seen in inelastic scattering could correspond to that level. This assignment is consistent with the angular distribution measured for the 7.71-MeV state in the ^{12}C(^{12}C, ^{6}He) ^{18}Ne reaction which has a shape similar to the one measured for the known 2^- state at $E_x = 5.45$ MeV.

The fact that only an upper limit for the inelastic scattering cross section could be determined in the region of the $E_{cm} = 3.2$ MeV ($E_x = 7.05$ MeV) is consistent with a 4^+ assignment. A 4^+ state requires an outgoing orbital angular momentum of $l = 4$ which would imply a very small width for the inelastic channel ($\Gamma_{p'} \leqslant 2$ keV).

C. Determination of $\Gamma_{p'}$

For the three resonances at $E_x = 7.05$, 7.60, and 7.71 MeV a sufficient number of experimental quantities [total widths, (p,α) and (p,p') cross sections] are now available, allowing a determination of the partial widths Γ_p, $\Gamma_{p'}$, and Γ_α under the assumption that the radiative width Γ_γ is negligible and that direct contributions to the cross section are small.

From the cross sections on resonance

$$\sigma_\alpha(E=E_r) = \frac{\omega\cdot\pi}{k^2}\cdot\frac{4\Gamma_p\Gamma_\alpha}{\Gamma^2}, \tag{1}$$

$$\sigma_{p'}(E=E_r) = \frac{\omega\cdot\pi}{k^2}\cdot\frac{4\Gamma_p\Gamma_{p'}}{\Gamma^2}, \tag{2}$$

and the total width Γ

$$\Gamma = \Gamma_p + \Gamma_{p'} + \Gamma_\alpha \tag{3}$$

one can solve for the partial widths Γ_p, $\Gamma_{p'}$, and Γ_α. In Eqs. (1) and (2) k is the wave number and ω the spin-statistical factor,

$$\omega = \frac{2J+1}{(2I_1+1)(2I_2+1)}, \tag{4}$$

with J the spin of the resonance and I_1 and I_2 the spins of the two particles in the entrance channel, respectively. The cross sections on resonance have to be corrected for the finite target thickness and for effects of the energy distribution of the beam.

For the proton width Γ_p one obtains from Eqs. (1)–(3)

$$\Gamma_p = \frac{\Gamma}{2}\cdot\left[1 \pm \sqrt{1-\left(\frac{\sigma_\alpha k^2}{\omega\pi}+\frac{\sigma_{p'}k^2}{\omega\pi}\right)}\right] \tag{5}$$

and similar expressions for $\Gamma_{p'}$ and Γ_α. The unitarity limit for the reaction cross section

$$\sigma_r = \sigma_\alpha + \sigma_{p'} \leq \omega\cdot\frac{\pi}{k^2} \tag{6}$$

ensures that the square root in Eq. (5) remains real.

Among the two possible solutions of Eq. (5) the one corresponding to the smaller alpha width was chosen, since the spectroscopic factors in the mirror nucleus ^{18}O are typically less than 0.1. The parameters obtained for the resonances are summarized in Tables I–III. Also included are states between $E_x = 6-7$ MeV which were recently reported in a study of ^{17}F(p,p) scattering, using a thick target technique [11]. With the spin assignment for the 6.15-MeV state from Ref. [11], values for the resonance strength and the width Γ_α have been extracted from our earlier [5] (p,α) measurement, although with quite large uncertainties.

It can be seen from Table II that the inelastic proton widths for natural parity states above $E_x = 7$ MeV are generally quite small compared to the elastic width. Thus a measurement of the inverse reaction ^{17}F(p,α) ^{14}O provides a good estimate for the astrophysical reaction rate of the ^{14}O(α,p) reaction for these resonances.

TABLE I. Spins, energies, and Coulomb shifts for states in ^{18}Ne above $E_x = 6$ MeV.

J^π	$E_x(^{18}\text{Ne})$ [MeV]	$E_x(^{18}\text{O})$ [MeV]	$E_x(^{18}\text{O}) - E_x(^{18}\text{Ne})$ [keV]	E_{cm} [MeV]
1^-	6.15	6.198	48	2.23
3^-	6.29	6.404	114	2.37
2^-	6.35	6.351	0	2.43
4^+	7.05 ± 0.1	7.11	60	3.13 ± 0.1
2^+	7.37 ± 0.06	8.21	840	3.48 ± 0.06
1^-	7.60 ± 0.05	7.62	20	3.69 ± 0.05
(2^+)		8.21	610	
(3^-)		8.29	690	
2^-	7.71 ± 0.05	7.77	60	3.79 ± 0.05

D. Spin-parity assignments for resonances above 7 MeV in ^{18}Ne

The results from elastic and inelastic scattering together with the (p,α) cross sections allow for an update of the spin-parity assignments for states in ^{18}Ne above $E_x = 7$ MeV.

1. $E_x = 7.05$ MeV

Based on the excitation function for elastic scattering, the resonance at $E_x = 7.05$ MeV is assigned a spin-parity value of 4^+. This level is the analog of the 4^+ state at 7.11 MeV in ^{18}O. The small cross section for inelastic scattering is consistent with this assignment.

2. $E_x = 7.37$ MeV

Little information is available for the resonance at $E_x = 7.37$ MeV. Since resonances at 7.60 and 7.71 MeV appear to be the 1^- and 2^- analogs of the 7.616- and the 7.771-MeV states in ^{18}O (see below), the analog of the 7.37-MeV resonance in ^{18}Ne has to be at higher excitation energy in ^{18}O. Possible candidates are 5^- states at 7.864 and 8.125 MeV, a 3^+ or 4^- level at 7.977 MeV, a 1^- state at 8.038 MeV, or a 2^+ level at 8.213 MeV. The small Wigner limit for the alpha width eliminates the 5^- assignment and the fact that this state is populated in the (p,α) reaction rules out the 3^+,4^- spin values, thus favoring a 1^- assignment. However, in Ref. [6] Fortune and Sherr have argued that all known low-lying negative parity states show small Coulomb shifts ($\Delta \sim 60$ keV) which speaks against a 1^- assignment, since the shift would be an order of magnitude larger (668 keV). The remaining candidate, the analog of the 2^+ state at 8.213 MeV in ^{18}O, would yield a Coulomb shift of 843 keV, comparable to that observed for the 3^+ state ($\Delta = 817$ keV).

The Coulomb shifts between analog states fluctuate because of the variations in the radial extent of the wave functions. Relatively low Coulomb energies occur for levels where the valence neutron configurations are relatively ex-

TABLE II. Widths and resonance strengths for states in ^{18}Ne above $E_x = 6$ MeV.

J^π	E_x [MeV]	E_{cm} [MeV]	Γ [keV]	$\omega\gamma_{(p,\alpha)}$ [eV]	Γ_α [eV]	Γ_p [keV]	$\Gamma_{p'}$ [keV]
1^-	6.15	2.23	50[a]	$0.8^{+1.2}_{-0.5}$[b]	3.2^{+5}_{-2}[b]		
3^-	6.29	2.37	$\leqslant 20$[c]	0.2	0.34[c]		
2^-	6.35	2.43	50[a]				
4^+	7.05	3.13	90 ± 40	29 ± 10	40 ± 14	90 ± 40	<1
2^+	7.37	3.48	70 ± 60	18 ± 14	40 ± 30		
1^-	7.60	3.69	75 ± 20	255 ± 30	1000 ± 120	72 ± 20	<2
(2^+)					610 ± 70		
(3^-)					440 ± 50		
2^-	7.71	3.79	70 ± 30			59 ± 25	11 ± 5

[a]Reference [11].
[b]This work.
[c]Reference [4].

tended. The best-known example for this is the Thomas-Ehrmann shift first noted by the fact that the difference in binding energy for the first excited $\frac{1}{2}^+$ states in the ^{17}O-^{17}F mirror pair is 380 keV less than that for the $\frac{5}{2}^+$ ground states. Since ^{18}O and ^{18}Ne differ by two units of charge, the Coulomb energies should be about twice this amount. States with large *s*-wave components are expected to have especially low Coulomb energy differences. This would then imply that large $l=0$ partial widths should be correlated with Coulomb energy differences that are about 800 keV lower than for other states. As pointed out in Ref. [6] these considerations result in even-parity states being much more likely to have low Coulomb energies than odd-parity ones. This argument can be used, in a probabilistic sense, to propose spin assignments relative to known states in ^{18}O.

3. E_x=7.60 MeV

The 7.60-MeV resonance is strongly populated in the (p,α) reaction. The shape of the angular distribution, however, is not very sensitive to the spin value of this level, allowing spin values between 1^- and 4^+. Because the only 2^+ and 4^+ levels available in this energy region have already been assigned to the 7.05- and the 7.37-MeV resonances, the 7.60-MeV resonance could have spin-parity values of 1^- or 3^-. The latter value would imply a Coulomb energy shift of 690 keV which is unlikely, as was discussed above. In addition, the 3^- mirror state in ^{18}O at $E_x = 8.29$ MeV has a considerably larger spectroscopic factor of 0.3 [12], which would imply a total width$\geqslant$1 MeV. Thus the 7.60-MeV resonance is likely to be the 1^- analog of the 7.616-MeV level in ^{18}O.

4. E_x=7.71 MeV

The resonance at 7.71 MeV, which is not seen in the (p,α) reaction, would then be the $J^\pi = 2^-$ analog of the 7.771-MeV 2^- state in ^{18}O. The structure of the excitation functions in the elastic channel is not sufficiently pronounced in this energy range to help in the spin-parity assignments, but it is consistent with these proposed spin-parity values (see Fig. 7). These new levels and their possible spin-parity assignments are also included in Fig. 5.

E. Comparisons with calculations

The extraction of parameters, such as the widths, from the measured elastic-scattering data using the *R*-matrix formalism of Ref. [10] is difficult because the excitation function has not been measured in sufficiently small energy steps. However, one can compare the excitation functions with *R*-matrix calculations for various spin assignments in order to restrict the choice of possible spin-parity values.

In order to determine the phase angles for potential scattering, the angular distributions at energies of $E_{cm} = 3.39$, 3.63, and 3.96 MeV (i.e., away from possible strong resonances) were fitted with the expression from the partial wave expansion (given in Ref. [13]) used to describe proton scattering from ^{16}O. The main difference for the ^{17}F+p experiment in this energy region was in the *s*-wave phase shift, which decreased from the hard-sphere value of $-45°$ to about $-85°$, as had also been observed in the neighboring system ^{16}O+p [13]. Without this change in the nonresonant phases the absolute cross sections were poorly described throughout this energy region. With the phase angles for po-

TABLE III. Spectroscopic factors $\Theta^2_{\alpha,p}$ for states with natural parity in ^{18}Ne and $E_x = 6$ MeV.

J^π	E_x [MeV]	$\Theta^2_\alpha(^{18}\text{Ne})$	$\Theta^2_\alpha(^{18}\text{O})$	$\Theta^2_p(^{18}\text{Ne})$
1^-	6.15	$0.19^{+0.3}_{-0.1}$[a]		
3^-	6.29	0.019[b]	0.023[b]	
4^+	7.05	0.50 ± 17	0.11	0.25
2^+	7.37	0.004 ± 0.003		
1^-	7.60	0.013 ± 0.0015	0.012	0.034
(2^+)		0.02 ± 0.0025	0.014	
(3^-)		0.07 ± 0.008	0.30	

[a]This work.
[b]Reference [4].

tential scattering fixed, the excitation functions for resonant scattering, calculated from the equations given in Ref. [10], are shown in Fig. 7. The calculations have been folded with an energy resolution of 100 keV. The solid line uses the resonance parameters tabulated in Tables I–III which give a good description of the experimental data. The dashed line assumes a 1^- assignment (rather than 4^+) for the 7.05-MeV state, in strong disagreement with the data, especially at backward angles.

IV. ASTROPHYSICAL IMPLICATIONS

With the resonance parameters summarized in Table II the astrophysical reaction rate can now be calculated. This rate is defined as the folding integral of the cross section with a Maxwell-Boltzmann distribution $f(v)$,

$$N_A\langle\sigma v\rangle = \int_0^\infty \sigma(v) f(v) dv. \tag{7}$$

For an isolated resonance with strength $\omega\gamma$ [see Eq. (1)] at energy E_r, this equation gives

$$N_A\langle\sigma v\rangle = 1.54\times 10^{11}(AT_9)^{-3/2}\times\omega\gamma\times\exp\left(-11.605\frac{E_r}{T_9}\right), \tag{8}$$

where N_A is Avogadro's number, A the reduced mass, and T_9 the temperature in units of 10^9 K.

The results are presented in Fig. 9. The rate for the breakout reactions is dominated by the resonance parameters for the 1^- state at 6.15 MeV which, because of its small strength, could be determined only with relatively large uncertainties in the present measurement (see shaded area in Fig. 9). Compared to this state, the contributions from the three higher-lying resonances (thin solid lines) are considerably smaller. It is only in the temperature range $T_9 \geqslant 3$ that they start to dominate the reaction rate. The thick solid line represents the sum of the 4^+, 2^+, and 1^- rates. Compared to the rates obtained in Ref. [4] we observe a good agreement for the 1^- state (not shown in Fig. 9), but a reduction of the contribution from the higher-lying resonances ($E_x = 7-8$ MeV) by a factor of 2–3 (see thick dot-dashed line and the inset in Fig. 9).

V. SUMMARY AND CONCLUSIONS

The astrophysical reaction rate for the ^{14}O(α,p) ^{17}F reaction of importance in various stellar environments such as x-ray bursts has, for the first time, been measured directly using a radioactive ^{17}F beam. From a measurement of the time-inverse ^{17}F(p,α) ^{14}O reaction resonance parameters for several states above an excitation energy of 7 MeV in ^{18}Ne could be determined. These data, together with measurements of excitation functions for elastic and inelastic scattering [^{17}F(p,p) ^{17}F and ^{17}F(p,p') ^{17}F$(1/2^+)$] were used to determine spin and parity values for four states in this energy region. These assignments differ from values given in earlier compilations. The results also indicate that the contribution of the ^{14}O(α,p) ^{17}F* reaction populating the first excited state in ^{17}F is small. The contribution of the resonances above $E_x = 7$ MeV to the astrophysical reaction rate is smaller than was previously assumed by a factor of 2–3.

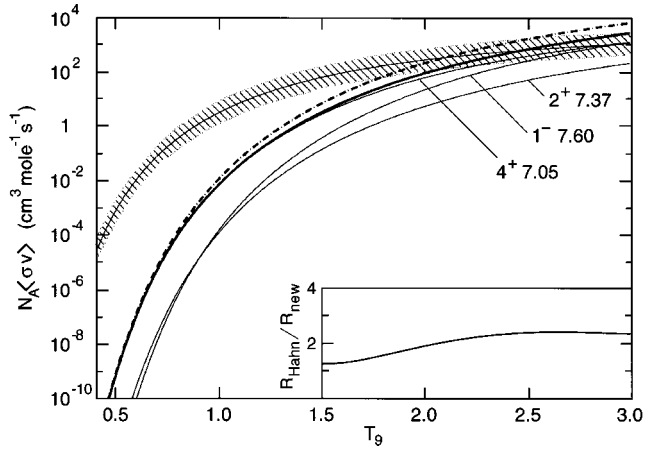

FIG. 9. Contributions to the astrophysical reaction rate from the states tabulated in Table II. The gray-shaded area represents the contribution from the 6.15-MeV, 1^- state. The thin solid lines are the contributions from the 4^+, 2^+, and 1^- states, respectively. The thick lines give the sum of the contributions of states in ^{18}Ne at $E_x = 7-8$ MeV from this work (solid line) and Ref. [4] (dot-dashed line), respectively. The insert shows the ratio of the reaction rates $R_{\text{Hahn}}/R_{\text{this work}}$.

ACKNOWLEDGMENTS

This work was supported by the U.S. D.O.E., Nuclear Physics Division, under Contract Nos. W-31-109-ENG-38(ANL), DE-FG02-98ER-41086(NU), and DE-FG02-91ER-40609 (Yale University). Oak Ridge National Laboratory is managed by the University of Tennessee for the U.S. D.O.E. under Contract No. DE-AC05-96OR22464.

[1] A. E. Champagne and M. Wiescher, Annu. Rev. Nucl. Part. Sci. **42**, 39 (1992).
[2] R. K. Wallace and S. E. Woosley, Astrophys. J., Suppl. Ser. **45**, 389 (1981).
[3] D. W. Bardayan *et al.*, Phys. Rev. Lett. **83**, 45 (1999).
[4] K. I. Hahn, *et al.*, Phys. Rev. C **54**, 1999 (1996).
[5] B. Harss *et al.*, Phys. Rev. Lett. **82**, 3964 (1999).
[6] H. T. Fortune and R. Sherr, Phys. Rev. Lett. **84**, 1635 (2000).
[7] B. Harss *et al.*, Rev. Sci. Instrum. **71**, 380 (2000).
[8] K. E. Rehm and F. L. H. Wolfs, Nucl. Instrum. Methods Phys. Res. A **273**, 262 (1988).

[9] D. R. Tilley, H. R. Weller, C. M. Cheves, and R. M. Chasteler, Nucl. Phys. **A595**, 1 (1995).
[10] J. M. Blatt and L. C. Biedenharn, Rev. Mod. Phys. **24**, 258 (1952).
[11] J. Gomez del Campo *et al.*, Phys. Rev. Lett. **86**, 43 (2001).
[12] The spectroscopic factor quoted in Phys. Rev. **111**, 277 (1958) is 0.2 due to a different definition of the single-particle value from that used in our paper.
[13] S. R. Salisbury and H. T. Richards, Phys. Rev. **126**, 2147 (1962).